Journal of Operation and Automation in Power Engineering

vol. 12, no. 2, Apr. 2024, Pages: 107-120

http://joape.uma.ac.ir

Improved Power System Dynamic Stability by DFIG in the Presence of SSSC Using Adaptive Nonlinear Multi-Input Backstepping

Z. Faramarzi , S. Abazari, S. Hoghoughi, N. R. Abjadi*

Faculty of Engineering, Shahrekord University, Shahrekord, Iran

Abstract— *In this paper, Doubly Feed Induction Generator (DFIG) improves the dynamic stability of the power system in the presence of Static Synchronous Series Compensator (SSSC) using nonlinear control theory. The control method used in this study is based on the nonlinear multi-input adaptive backstepping control. The control signals are assigned to DFIG and SSSC and synchronous generator excitation system. The applied control method is more effective than the conventional linear and nonlinear ones which are reported in the literature. Also in this study, control inputs are designed considering their appropriate constraints. The controller coefficients are optimally selected using intelligent algorithms that increase the performance of the controller in terms of achieving stability. The designed control is robust against parameter variations and load changes as well as changing in the location of the disturbances. This method is simulated in two aspects of the synchronous machine model as a third-order model and a second-order one. The methods are implemented on a 39-bus IEEE system and the simulation results show the effectiveness of the proposed control mechanism.*

Keywords—Dynamic stability, DFIG, SSSC, Multi-input adaptive backstepping, Intelligent algorithm

1. INTRODUCTION

In todays' industrial world, the expansion of the use of wind energy as one of the sources of renewable energies has become more common. This is due to the growth of technology, good infrastructure, lower comparative costs, reduced emissions and abundant availability of this type of energy. Variable nature of wind energy paved the way to implement variable speed machines, especially DFIGs. As a result, DFIGs have become one of the most important wind energy utilization systems. Their use in wind energy conversion systems has been greatly increased due to the advantages such as low cost, small size, ability to generate maximum power in different wind speed conditions, elimination of external DC sources, separation control of active and reactive powers and smaller scale need of applied converters [2]. The growing influence of DFIGs in power networks has led to the issue of the stability of the power systems. A fuzzy control law for monitoring active and reactive powers of DFIG is designed in [3]. In [4], to mitigate the sub synchronous resonance, using fuzzy method, a supplementary signal is used in DFIG control. In [5], the pitch angle in wind turbine based DFIG is controlled using fuzzy logic method. The dynamic energy stability region of DFIG-integrated power system is investigated in [6]. If the DFIG system is not properly controlled, variations in wind speed with unpredictable loads or changing connections can put a lot of stress on the wind power systems, [7, 8].

Flexible AC Transmission Systems (FACTSs) are used to facilitate power transmission and to increase transmission lines capacity. FACTS devices have been widely implemented in the last two decades to strengthen the structure of modern power systems. With the advent of FACTS elements such as SSSC, dramatic changes are taking place in the transmission networks in terms of improved performance and power systems stability, [9, 10]. In [11], power system stability is enhanced using SSSC with a fractional order controller.

Stability is one of the first requirements in power systems. A suitable power system should be robust to errors and unwanted factors. Moreover, it should ensure the stability from different aspects. Types of errors, short circuits, load growth, production shortages and many other factors are serious threats to system immunity and disruption of stability. One of these phenomena is low-frequency oscillations, which occur mostly in the face of small and sudden disturbances. Power systems are highly nonlinear, complex, and interconnected systems that are under constant pressure to respond to increased consumer demand. For this reason, the study of stability is a very important issue which leads to the improved performance, efficiency and reliability of power systems [12].

Power networks excitation control systems can provide additional damping through the design of Power System Stabilizers (PSS) to improve the stability [13]. In this type of damping controllers, the local linear model of the power system around the operating point is often used and different linear control methods are developed and applied. However, these methods do not result in the required necessary performance in the case of faults. To improve the performance of the power system, some studies have implemented a combination of linear and nonlinear controllers [14]. The nonlinear control methods such as backstepping control, adaptive control, adaptive backstepping control, sliding mode control and Lyapunov direct method have been widely used to improve the stability of power systems; however, these methods are more based on improving damping by controlling the excitation system of generators [15, 16]. Due to the growing penetration of wind energy sources in power systems and the fact that DFIGs have the ability to stabilize the voltage in their vicinity in the event of disturbances, they can be used beneficially for the stability of the power system and therefore they can have a share of network stability. However, in most studies, this potential DFIGs capability has not been noticed for improved stability and more attention

Received: 27 Mar. 2022
Revised: 19 Jul. 2022
Accepted: 08 Sep. 2022
*Corresponding author:
E-mail: saeedabazari@yahoo.com (S. Abazari)
DOI: 10.22098/joape.2023.10565.1753
Research Paper

Table 1. The name of each of the variables used in the equations

symbol	Variable name	symbol	Variable name
δ_{0i}	Rotor angle of i-th generator in steady state	δ_i	Rotor angle of i-th generator
ω_{0i}	Rotor speed of i-th generator in steady state	ω_i	Rotor speed of i-th generator
V_i	Amplitude of Generator terminal voltage i-th	$\acute{E}_{qi}$	Internal voltage of i-th generator in q-axes
θ_i	Phase of Generator terminal voltage i-th	$\acute{E}_i$	Internal voltage of i-th generator
$\acute{T}_{d0i}$	Constant time generator excitation coil i-th	I_{di}	Stator current of i-th generator in d-axis
x_{di}	d-axis reactance generator steady state i-th	I_{qi}	Stator current of i-th generator in q-axis
$\acute{x}_{di}$	d-axis reactance generator transient state i-th	u_{fi}	Excitation voltage of i-th generator
x_{qi}	q-axis reactance generator steady state i-th	M_i	Moment of inertia of i-th generator
X_i	Equivalent Reactance of DFIG in steady state	P_{mi}	Mechanical input power of i-th i-th generator
$\acute{X}_i$	Equivalent Reactance of DFIG in transient state	u_d	Signal control of DFIG

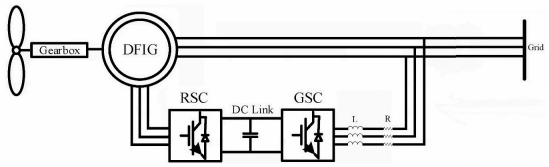

Fig. 1. DFIG with RSC and GSC Connected a Power System

has been paid to increasing the number of DFIGs to extract their maximum power. Hence, the use of DFIGs to improve the stability of the power grid should be more investigated [17, 18].

Investigating and improving the stability of large-scale power networks including synchronous generators and DFIGs in the presence of FACTS elements are one of the important challenges of the power systems [19, 20]. In [21], a STATCOM is used as a reactive support to regulate the main voltages in a power system with DFIG. In [22], the voltage stability of power system with DFIG using SSSC is improved. In [23], it is shown that connecting FACTS controllers improves the stability of the new power systems with the presence of DFIGs. In [24], the efects of three FACTS controllers including SSSC on the transient stability of a multi-machine power system based on a DFIG using linear conventional controllers are studied. It is worthwhile to note that the power system with SSSC and DFIG is a nonlinear system and conventional linear controls are not suitable for large changes in operating point and the effect of disturbances.

In this paper, the main concern is to consider simultaneous control of DFIG and SSSC together with synchronous generators excitation system to improve the dynamic stability of a power system. The proposed scheme is to apply nonlinear multi-input adaptive backstepping method. This designed control method is more effective than conventional linear and nonlinear ones. Also in this study, controller coefficients are optimally selected using intelligent algorithms considering control inputs limitations, which increases the effectiveness of the controller in terms of achieving stability. The designed control is robust against changing parameters and load variations as well as changing the location of the disturbances. The proposed method has been implemented considering two synchronous machine models namely 3rd -order and 2nd-order ones. In the 2nd-order model of synchronous generator, stability improvement is done only by DFIG and SSSC control signals. In other words, if the excitation system of synchronous generators is deactivated for any reason, the dynamic stability of the power system can be realized by using the existing control signals.

In the following, first the DFIG model and then the power injection model for SSSC are presented. In the presented approach, synchronous generators are modeled by a 3rd -order and 2nd-order mathematical relations. Then, a multi-input backstepping control law is developed for the two mentioned case studies, and at the end, the simulation results for these case studies are presented. Moreover, a comparison is made with conventional methods.

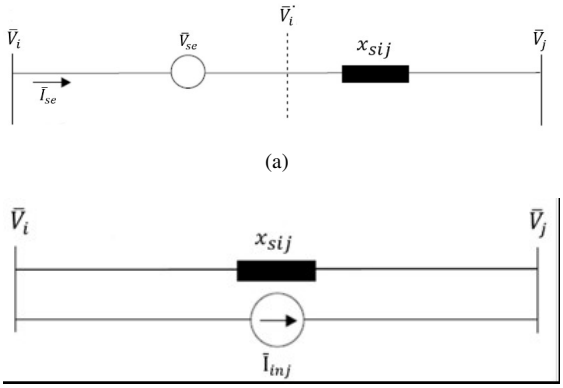

Fig. 2. (a) SSSC between bus i and bus j, (b) equivalent circuit of SSSC

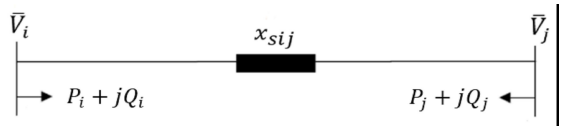

Fig. 3. Alternative equivalent injection model of SSSC in power system

2. Power System Modeling

In this section, the assumed model for DFIG is firstly introduced. Then the implemented model for SSSC is defined. Finally, the model of the overall power system including DFIG, SSSC and synchronous machines will be presented.

2.1. DFIG Model

Fig. 1 shows a DFIG connected to the power grid. The DFIG has two power electronics converters namely Rotor-Side-Converter (RSC) and Generator-Side-Converter (GSC). It is worthwhile to note that the improvement of dynamic stability in power system is the main concern in this study. The RSC has the key role on this issue. Therefore, in the presented model, the RSC inputs are the control variables. The considered model is known as the synchronous generator model for DFIG. In this model, the stator resistance is assumed to be zero. Based on this model, the 3^{rd} -order state equations are developed as follows [25]:

$$\begin{cases} \dot{\delta}_i = \frac{1}{\acute{E}_{qi} T_{0i}}(-T_{0i}(\omega_i - \omega_0)\acute{E}_{qi} \\ -\frac{X_i - \acute{X}_i}{\acute{E}_{qi} T_{0i}} V_i sin(\delta_i - \theta_i) + T_{0i}\omega_0 V_{ri} cos(\delta_i - \Phi_{ri})) \\ \dot{\omega}_i = \frac{\omega_0}{2H_i}[P_{mi}\frac{\omega_s}{\omega_i} - B_{ij}\acute{E}_{qi}V_i sin(\delta_i - \theta_i)] \\ \dot{\acute{E}}_i = \frac{1}{T_{0i}}(-\frac{X_i}{\acute{X}_i}\acute{E}_{qi} + \frac{X_i - \acute{X}_i}{\acute{X}_i} V_i cos(\delta_i - \theta_i) + \\ T_{0i}\omega_0 V_{ri} cos(\delta_i - \Phi_{ri})) \end{cases} \quad (1)$$

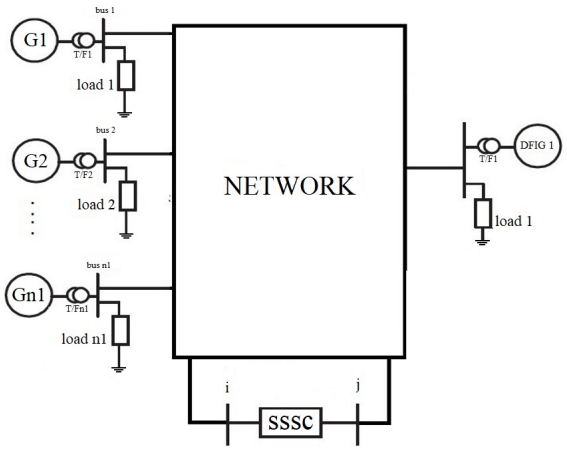

Fig. 4. Overview of the Power Network under Study

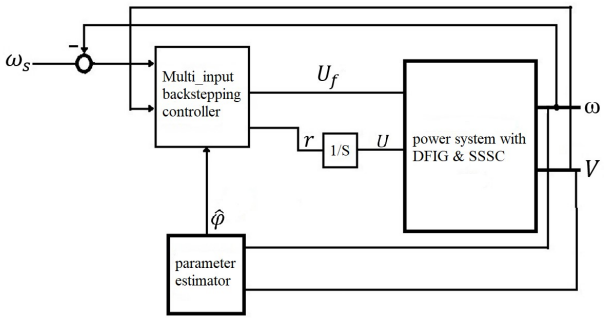

Fig. 5. Adaptive Control Diagram for Power System Including DFIG and SSSC

In the above equations, V_i and θ_i are amplitude and phase angle of each bus voltage, respectively. B_{ij} is the imaginary part of the admittance matrix which exists between DFIG and the connected bus. $\acute{E}_i$ is the internal voltage of i-th generator. V_{ri} and Φ_{ri} are amplitude and phase angle of applied voltage to rotor in polar coordinates, respectively.

2.2. The Injected Model of SSSC

To model the SSSC element in the power grid, it is assumed that each SSSC element in the grid is located between bus *i* and bus *j* as shown in Fig. 2. The model proposed for SSSC is a series converter. This converter can inject reactive power into the series branch and can be used to stabilize the voltage of the power system buses as well as to contribute to the improvement of dynamic stability [26].

SSSC function is implemented to improve dynamic stability by choosing the appropriate series voltage source, that is, V_{se}. Hence, this controllable voltage of the converter can be represented as in (2):

$$\begin{cases} \bar{\mathrm{I}}_{inj} = -jB_{ij}V_{se}v_{se} = V_{se}e^{j\Phi_{se}} \\ B_{ij} = \frac{1}{x_{sij}} \end{cases} \tag{2}$$

In Fig. 3, P_{si}, P_{sj}, Q_{si} and Q_{sj} are defined between bus i-th and bus j-th as below:

$$\begin{cases} S_i = P_{si} + jQ_{si} = -B_{ij}V_{sek}V_i sin\,(\theta_i - \Phi_{sek}) \\ \quad +jB_{ij}V_{sek}V_i cos\,(\theta_i - \Phi_{sek}) \\ \\ S_j = P_{sj} + jQ_{sj} = B_{ij}V_{sek}V_j sin\,(\theta_j - \Phi_{sek}) \\ \quad -jB_{ij}V_{sek}V_j cos\,(\theta_j - \Phi_{sek}) \end{cases} \tag{3}$$

In this study, it is assumed that SSSC component only produces and consumes reactive power. It is also assumed that the series resistance of the transmission line, on which, the SSSC is located equals zero. Hence, the SSSC voltage angle will be determined in the following form:

$$\Phi_{sek} = tan^{-1}\left(\frac{V_j sin\,(\theta_j) - V_i sin\,(\theta_i)}{-V_j cos\,(\theta_j) + V_i cos\,(\theta_i)}\right) \tag{4}$$

2.3. Modeling of the Overall Power System Including DFID and SSSC

Fig. 4 shows an overview of the power network under study. The target network includes n1 synchronous generator, one DFIG and one SSSC. Here the transmission lines are considered lossless and are represented by the admittance matrix $\overline{Y}_{ij} = jB_{ij}$. In the power system, it is assumed that the mechanical input power of the generators is constant. Moreover, the stator resistance of the generators is ignored. The total load on each bus *i* is modeled as $Y_i = G_i - jB_i$.

Firstly, the model of synchronous generators is represented as a 3^{rd} -order model according to (6). In this model, u_{fi} is considered as the control input of the generator internal voltage excitation circuit [12].

$$\begin{cases} \dot{\delta}_i = \omega_i - \omega_0 \\ \dot{\omega}_i = \frac{1}{M_i}[P_{mi} - P_{ei}] \\ \dot{E}_{qi} = \frac{1}{\acute{T}_{d0i}}(u_{fi} - \acute{E}_{qi} - (x_{di} - \acute{x}_{di})I_{di} \end{cases} \tag{5}$$

$$P_{ei} = \frac{\acute{E}_{qi}V_i sin(\delta_i - \theta_i)}{\acute{x}_{di}} + \frac{V_i{}^2 sin2(\delta_i - \theta_i)(\acute{x}_{di} - x_{qi})}{2x_{qi}\acute{x}_{di}} \tag{6}$$

$$I_{di} = \frac{\acute{E}_{qi} - V_i cos(\delta_i - \theta_i)}{\acute{x}_{di}} \tag{7}$$

A 3^{rd} -order model for synchronous generators is assumed to be adequate for dynamic stability analysis in this study. Higher order models have more damping effect in their nature. This fact makes the dynamic stability improvement to be easier to achieve with respect to lower-order models. Hence, a suitable and realistic choice for modelling the synchronous generators is a 3^{rd} -order or a 2^{nd}-order form to challenge the desired improvement in dynamic stability.

Next, the model of synchronous generators is considered as a 2^{nd}-order model. In this model, the internal voltage of synchronous generators is assumed to be constant. Therefore, equation (8) exhibits this reduced-order case:

$$\begin{cases} \dot{\delta}_i = \omega_i - \omega_0 \\ \dot{\omega}_i = \frac{1}{M_i}[P_{mi} - \acute{E}_{qi}I_{qi}] \end{cases} \tag{8}$$

The algebraic equations of power balance in all buses connected to the synchronous generators and buses connected to SSSC and DFIG of power system results in the following equations:

$$\begin{cases} P_{Li} + \int_{j=1}^{N} B_{ij}V_iV_j sin\,(\theta_i - \theta_j) = 0 \\ -Q_{Li} + \int_{j=1}^{N} B_{ij}V_iV_j cos\,(\theta_i - \theta_j) = 0 \end{cases} \tag{9}$$

where, N is the total number of buses including synchronous generator, DFIG and buses connected to SSSC. Note that N = n + 2, where n equals to the total number of synchronous generators and DFIG, n = n1 + 1. $B'_{ij}s$ are the elements of the reduced order admittance matrix. The SSSC control inputs are defined as $u_{s1} = V_{sek}cos\,(\Phi_{se})$ and $u_{s2} = V_{se}sin\,(\Phi_{se})$. With trigonometric expansion in algebraic equations of the power balance in the i-th and j-th buses and differentiating and separating the variables, the following equation is obtained:

$$\begin{bmatrix} a_{1,1} & \cdots & a_{1,2(n+2)} \\ \vdots & \ddots & \vdots \\ a_{2N,1} & \cdots & a_{2N,2(n+2)} \end{bmatrix} \begin{bmatrix} \dot{V}_1 \\ \vdots \\ \dot{V}_{n+2} \\ \vdots \\ \dot{\theta}_1 \\ \vdots \\ \dot{\theta}_{n+2} \end{bmatrix} = - \begin{bmatrix} b_{1,1} & \cdots & b_{1,2n} \\ \vdots & \ddots & \vdots \\ b_{2N,1} & \cdots & b_{2N,2n} \end{bmatrix} \begin{bmatrix} \dot{E}_{q1} \\ \dot{E}_{q2} \\ \vdots \\ \dot{E}_{qn} \\ \dot{\delta}_1 \\ \dot{\delta}_2 \\ \vdots \\ \dot{\delta}_n \end{bmatrix} - \begin{bmatrix} g_{1,1} & g_{1,2} \\ \vdots & \vdots \\ g_{2N,1} & g_{2N,2} \end{bmatrix} \begin{bmatrix} \dot{u}_{s1} \\ \dot{u}_{s2} \end{bmatrix} \tag{10}$$

where the definitions of a_{ij}, b_{ij} and g_{ij} are given in Appendix A. Equation (10) can be rewritten as the following compact form

$$\begin{bmatrix} A \end{bmatrix} \begin{bmatrix} \dot{V} \\ \dot{\theta} \end{bmatrix} = - \begin{bmatrix} B \end{bmatrix} \begin{bmatrix} \dot{E}_q \\ \dot{\delta} \end{bmatrix} - \begin{bmatrix} G \end{bmatrix} \dot{U}_s \tag{11}$$

where $\dot{V} = \begin{bmatrix} \dot{V}_1 \, .. \dot{V}_{n+2} \end{bmatrix}^T$, $\dot{\theta} = \begin{bmatrix} \dot{\theta}_1 . . \dot{\theta}_{n+2} \end{bmatrix}^T$, $\dot{E}_q = \begin{bmatrix} \dot{E}_{q1} \, .. \dot{E}_{qn1} \quad \dot{E} \end{bmatrix}^T$, $\dot{\delta} = \begin{bmatrix} \dot{\delta}_1 \, .. \dot{\delta}_{n1} \quad \dot{\delta}_d \end{bmatrix}^T$ and $\dot{U}_s = \begin{bmatrix} \dot{u}_{s1} \\ \dot{u}_{s2} \end{bmatrix} = \begin{bmatrix} r_1 \\ r_2 \end{bmatrix} = r$.

Since r_1 and r_2 are interdependent, there is practically only one control input for SSSC.

Using (11) and defining $\dot{\delta}_n$ and $\dot{E}_{qi}$ in (1) and (5) together with defining $h_i = \frac{1}{T_{0i}}(-\acute{E}_{qi} - \left(X - \acute{X}\right) I_{di})$, equation (13) will be obtained.

$$\dot{E}_{qi} = h_i + \frac{1}{T_{0i}} u_{fi} \tag{12}$$

$$\begin{bmatrix} A \end{bmatrix} \begin{bmatrix} \dot{V} \\ \dot{\theta} \end{bmatrix} = - \begin{bmatrix} B \end{bmatrix} \begin{bmatrix} h_i \\ \dot{\delta} \end{bmatrix} - \begin{bmatrix} \acute{B} \end{bmatrix} U_f - \begin{bmatrix} G \end{bmatrix} r,$$
$$\acute{B} = \begin{bmatrix} B \end{bmatrix} \begin{bmatrix} \frac{1}{T_{01}} & \cdots & \frac{1}{T_{0n}} 0 & \cdots & 0 \end{bmatrix}^T \tag{13}$$

In the above equation, $U_f = \begin{bmatrix} u_{f1} & \cdots u_{fn1} & u_{d1} & u_{d2} \end{bmatrix}^T$ is corresponding to the excitation of synchronous generators and $\dot{U}$ is the controllable input of SSSC. By solving the matrix equation (13), it is obtained that

$$\begin{bmatrix} \dot{V} \\ \dot{\theta} \end{bmatrix} = \overbrace{-[A]^{-1}[B]}^{C} \begin{bmatrix} h_i \\ \omega - \omega_0 \end{bmatrix} \overbrace{-[A]^{-1}\left[\acute{B}\right]}^{D} U_f \overbrace{-[A]^{-1}[G]}^{K} r \tag{14}$$

with the following forms

$$C = \begin{bmatrix} c_{1,1} & \cdots & c_{1,2(n+1)} \\ \vdots & \ddots & \vdots \\ c_{2N,1} & \cdots & c_{2N,2(n+1)} \end{bmatrix},$$
$$D = \begin{bmatrix} d_{1,1} & \cdots & d_{1,n+1} \\ \vdots & \ddots & \vdots \\ d_{2N,1} & \cdots & d_{2N,n+1} \end{bmatrix},$$
$$K = \begin{bmatrix} k_{1,1} & \cdots & k_{1,2} \\ \vdots & \ddots & \vdots \\ k_{2N,1} & \cdots & k_{2N,2} \end{bmatrix}, \tag{15}$$
$$H = \begin{bmatrix} h_i \\ \omega \end{bmatrix}$$

Finally, the power system state equations with DFIG and SSSC are expressed in (16):

$$\begin{aligned} \dot{\delta}_i &= \omega_i - \omega_{0i} \\ \dot{\omega}_i &= \tfrac{1}{M_i}[P_{mi} - P_{ei}] \quad (16-a) \\ \dot{E}_{qi} &= f_{gi}(x) + g_{gi}(x) u_{fi} \end{aligned}$$

$$\begin{aligned} \dot{\delta}_i &= (\omega_i - \omega_{0i}\ ) \\ \dot{\omega}_i &= \tfrac{\omega_0}{2H_i}[P_{mi}\tfrac{\omega_s}{\omega_i} - B_i \acute{E}_i V_i sin(\delta_i - \theta_i)] \end{aligned} \tag{16b}$$

$$\begin{aligned} \dot{E}_i &= f_{di}(x) + g_{di}(x) u_{df1i} \\ \dot{V}_i &= \textstyle\int_{j=1}^{n+p} c_{ij} H_j + \int_{j=1}^{n+p} d_{ij} u_{fj} + \int_{j=1}^{n+p} k_{ij} r (16 - c) \\ \dot{\Phi}_i &= \textstyle\int_{j=1}^{n+p} c_{i+n+2,j} H_j + \int_{j=1}^{n+p} d_{i+n+2,j} u_{fj} + \int_{j=1}^{n+p} k_{i+n+2,j} r \end{aligned} \tag{16c}$$

Substituting the definitions of $I_{di}$and I_{qi} from (6) and (7) leads to obtain the equations represented in (16). The definitions of f_{di}, g_{di}, f_{di} and g_{di} are given in Appendix A. The first part is related to synchronous generators, the second part is related to DFIGs and the third part is related to network buses voltages.

3. Nonlinear Controller Design

Using the obtained model to improve the dynamic stability of the power system, control inputs are designed in [27]. Due to the fact that two models for synchronous generators are considered, the control inputs are designed separately.

3.1. Controller Design for SSSC and DFIG Considering 3^{rd} -Order and 2^{nd}-order Models for Synchronous Generators

In this case, considering that the 3^{rd} -order model for synchronous generators is applied, the number of control inputs of the system equals to n + 2. One of these inputs is related to SSSC and one is related to DFIG and the remaining ones are related to the excitation current of synchronous generators. Here, the SSSC input is used separately to improve the voltage profile by feedback linearization control on one of the buses connected to the SSSC. Other inputs are used to improve the dynamic stability after fault clearance by the multi-input backstepping control.

From (16), the derivative of SSSC voltage amplitude is given by [28]:

$$\dot{V}_m = \int_{j=1}^{N} c_{mj} H_j + \int_{j=1}^{N} d_{mj} u_{fj} + \int_{j=1}^{N} k_{mj} r \tag{17}$$

where m is the bus number connected directly to SSSC which should be regulated. Based on feedback linearization control the following control law is obtained:

$$\begin{aligned} r = \frac{1}{\int_{j=1}^{n+p+2} k_{mj}} \Big[& - \int_{j=1}^{N} c_{mj} H_j - \int_{j=1}^{N} d_{mj} u_{fj} \\ & - k_{v1}(V_m - V_{md}) \ - k_{v2} \Big] \end{aligned} \tag{18}$$

where V_{md} is the desired bus voltage which should be regulated. V_{md} is constant; so

$$\dot{V}_{md} = 0.$$

In the following, the mathematical form of the adaptive backstepping control will be explained

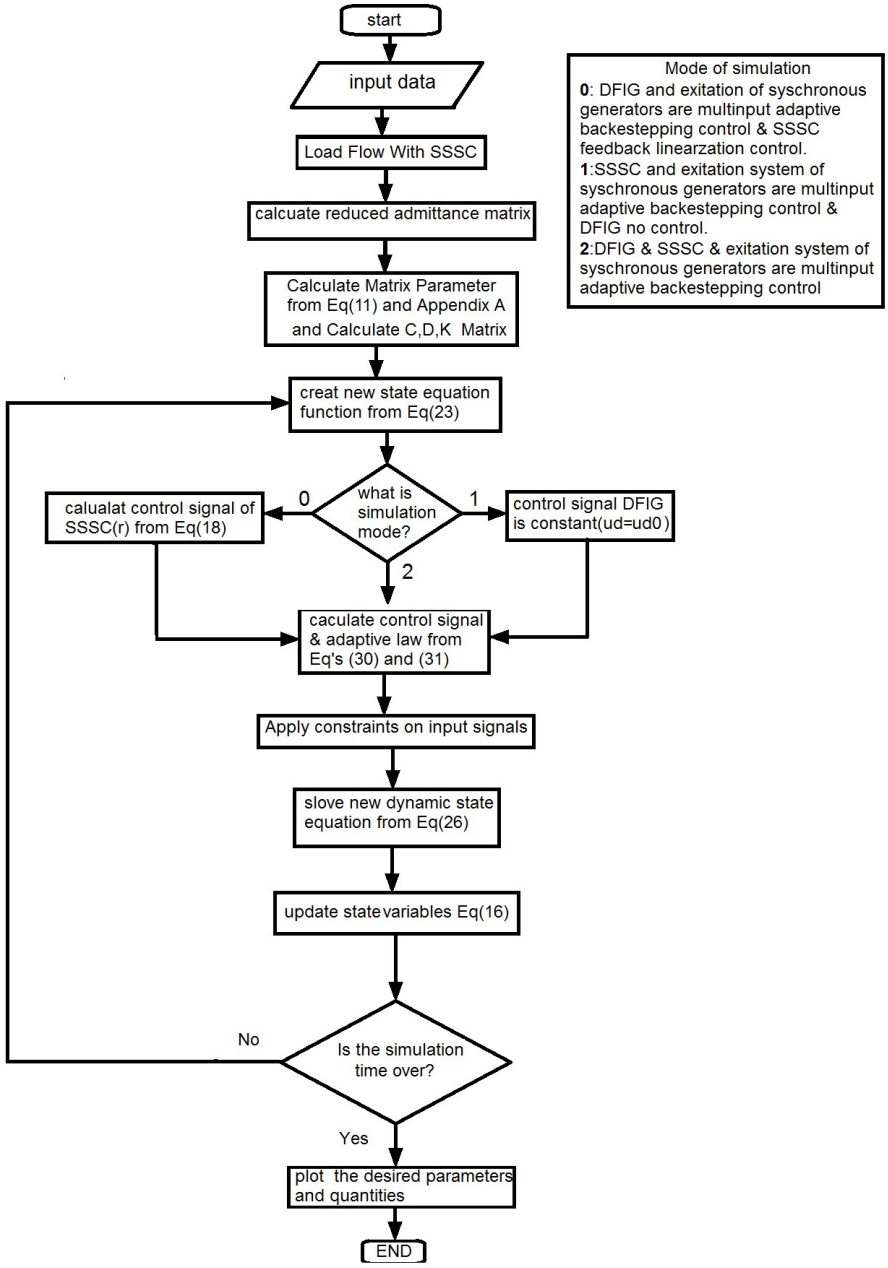

Fig. 6 (a). Power system Control Flowchart Including SSSC and DFIG with 3^{rd}-order Model of Synchronous Generators with Multi-Input Adaptive Backstepping Control Method

Let consider the following strict feedback system

$$\begin{aligned}
\dot{x}_1 &= x_2 + \varphi_1(x_1)^T\theta \\
\dot{x}_2 &= x_3 + \varphi_2(x_1, x_2)^T\theta \\
&\vdots \\
\dot{x}_{n-1} &= x_n + \varphi_{n-1}(x_1, x_2, \ldots, x_{n-1})^T\theta \\
\dot{x}_n &= u + \varphi_n(x_1, x_2, \ldots, x_n)^T\theta
\end{aligned} \tag{19}$$

where $x_i \in R$ are state variables; i=1,2,..,n; $\theta \in$Rp is the uncertain parameters vector; φ_i are differentiable function of order n-th and $\varphi_i(0,\ 0,\ \ldots,\ 0) = 0$; u$\in$ R is the control input.

With the assumed conditions, the control input is obtained in the form of (20) and the adaptation law of uncertain parameters is represented in the form of (21).

$$\begin{aligned}
u = \alpha_n = &-z_{n-1} - c_n z_n - {\varphi_n}^T\hat{\theta} \\
&+ \int_{j=1}^{n-1} \frac{d\alpha_{n-1}}{dx_j} x_{j+1} + \frac{d\alpha_{n-1}}{d\hat{\theta}}\dot{\hat{\theta}} + \beta_n
\end{aligned} \tag{20}$$

$$\dot{\hat{\theta}} = \Gamma \int_{i=1}^{n} z_i \varphi_i \tag{21}$$

Details of this method and the definition of its variables are presented in [29]. The method described in [29] is used for a single-input system. Here, by developing the method used for a multi-input system, a multi-input backstepping controller is designed for the power system with a 3^{rd} -order synchronous generator model. For this purpose, the equations must have a similar form as presented in (19). In this regard, first the new state

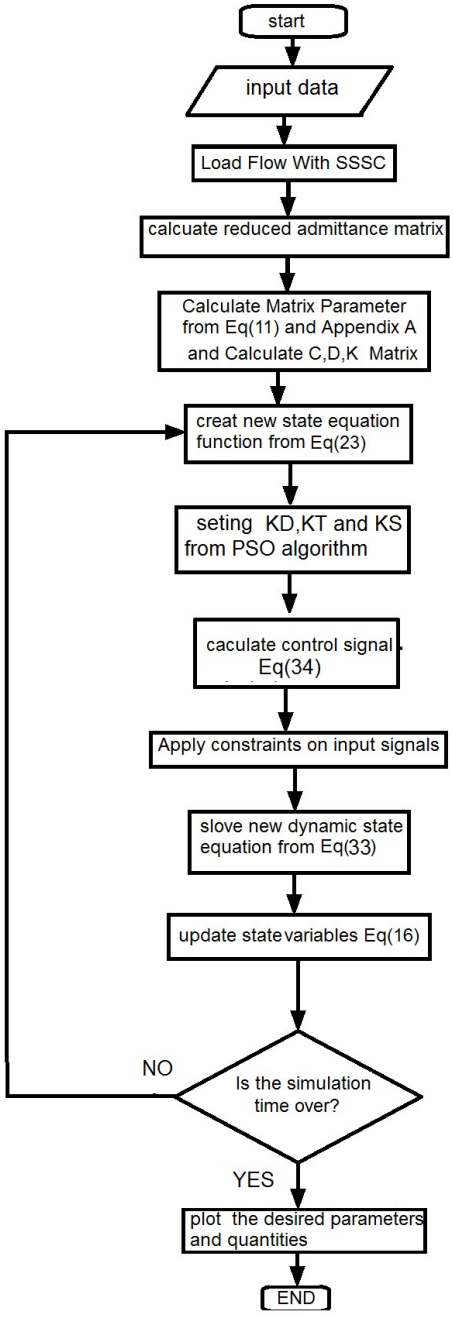

Fig. 6 (b). Power System Control Flowchart Including SSSC and DFIG with 2^{nd}-order Model of Synchronous Generators with Multi-Input Adaptive Backstepping Control Method

variables are defined as in (22).

$$x_{1i}=\delta_i-\delta_{i0}\ ,x_{2i}=\omega_i-\omega_{0i}$$

$$x_{3i}=\begin{cases}\frac{\acute{E}_{qi}V_i sin(\delta_i-\theta_i)}{\acute{x}_{di}}+\frac{{V_i}^2 sin2(\delta_i-\theta_i)}{2x_{qi}\acute{x}_{di}} 1<i<n_1\\ B_i\acute{E}_i V_i sin(\delta_i-\theta_i)\ for\ i=\ n\end{cases} \quad (22)$$

After substituting the definitions (22) in (16), the general form of the equations for each generator is obtained as follows:

$$\begin{cases}\dot{x}_{1i}=x_{2i}\\ \dot{x}_{2i}=\frac{1}{M_i}[P_{mi}-x_{3i}]\\ \dot{x}_{3i}=f_{Ti}+\Gamma_i\varphi_i+\int_{j=1}^{n+2}g_{Tij}u_{fj}+\int_{j=1}^{n+2}L_{ij}r\end{cases} \quad (23)$$

The above dynamic equations have a suitable form for controller design by adaptive backstepping method. In this relation $x_{di}-\acute{x}_{di}=\varphi_i$ acts as an uncertain parameter and Γ_i is a function of system variables.

$\Gamma_i(x)=-\frac{\acute{E}_{qi}-V_i cos(\delta_i-\theta_i)}{\acute{T}_{d0i}\acute{x}_{di}}$ 1<i<n1

$\Gamma_i(x)=\frac{1}{T_{0i}\acute{X}_i}\left[V_i cos(\delta_i-\theta_i)-\frac{V_i cos(\delta_i)sin(\delta_i-\theta_i)}{sin(\delta_i)}\right]$; n1+1<i<n

The matrix form of (23) is rewritten obtained as in (24)

$$\begin{cases}\dot{X}_1=X_2\\ \dot{X}_{2i}=M_{inv}[P_m-X_3]\\ \dot{X}_{3i}=F_T+U+\Gamma\varphi\end{cases} \quad (24)$$

where

$$U=G_T U_f+Lr$$
$$Z_1=[z_{11}\ \ z_{12}\ \ \dots\ z_{1n}]^T,\ Z_2=[z_{21}z_{22}\ \ ..\ \ z_{2n}]^T$$
$$X_1=[x_{11}\ \ x_{12}\ \ \dots\ x_{1n}]^T,\ X_2=[x_{21}x_{22}\ \ ..\ \ x_{2n}]^T$$
$$X_3=[x_{31}\ \ x_{32}\ \ \dots\ x_{3n}]^T,\ X_{3s}=[x_{3s1}x_{3s2}\ \ ..\ \ x_{3sn}]^T$$
$$\varphi=[x_{d1}-\acute{x}_{d1}\ \ x_{d2}-\acute{x}_{d2}\ \ \dots\ x_{dn}-\acute{x}_{dn}]^T$$
$$\Gamma=\begin{bmatrix}\Gamma_1(X_1,X_2,X_3) & \cdots & 0\\ \vdots & \ddots & \vdots\\ 0 & \cdots & \Gamma_n(X_1,X_2,X_3)\end{bmatrix}$$

The following variables are defined based on the backstepping method:

$$Z_1=X_2+K_D X_1 Z_2=X_3-X_{3s} \quad (25)$$

The derivatives of these variables are obtained as:

$$\dot{Z}_1=M_{inv}[P_m-X_3]+K_D(Z_1-K_D X_1)$$
$$\dot{Z}_2=F_T+U+\Gamma\varphi-\dot{X}_{3s} \quad (26)$$

Now a Lyapunov function is considered as follows:

$$V_L={X_1}^T X_1+{Z_1}^T Z_1+{Z_2}^T Z_2+\widetilde{\varphi}^T\widetilde{\varphi}$$

where $\widetilde{\varphi}=\varphi-\widehat{\varphi}$ and $\widehat{\varphi}$ is the estimated value of φ.

$$\dot{V}_L={X_1}^T\dot{X}_1+{Z_1}^T K_T\dot{Z}_1+{Z_2}^T K_S\dot{Z}_2+\widetilde{\varphi}^T\gamma\dot{\widetilde{\varphi}}$$

Substituting from (24) and (26), one can obtain

$$\begin{aligned}\dot{V}_L=&{X_1}^T(Z_1-K_D X_1)\ +{Z_1}^T(M_{inv}[P_m-X_3]+K_D X_2)\\ &+{Z_2}^T(F_T+U+\Gamma\varphi-\dot{X}_{3s})+\widetilde{\varphi}^T\gamma\dot{\widetilde{\varphi}}\ )\\ =&-{X_1}^T K_D X_1+{Z_1}^T(X_1+M_{inv}[P_m-X_{3s}]+K_D X_2)\\ &+{Z_2}^T(F_T+U+\Gamma\widehat{\varphi}-M_{inv}\ Z_1-\dot{X}_{3s})\\ &+({Z_2}^T\Gamma+\dot{\widehat{\varphi}}^T\gamma)\widetilde{\varphi}\end{aligned}$$

Since the values of uncertain parameters are constant; $\dot{\varphi}=0$, then $\dot{\widetilde{\varphi}}=-\dot{\widehat{\varphi}}$. For the derivative of the Lyapunov function to be negative semi-definite, the following conditions must be met:

$$X_1+M_{inv}[P_m-X_{3s}]+K_D X_2)=-K_T Z_1 \quad (27)$$

$$(F_T+U+\Gamma\widehat{\varphi}-M_{inv}\ Z_1-\dot{X}_{3s})=-K_s Z_2$$
$$({Z_2}^T\Gamma+\dot{\widehat{\varphi}}^T\gamma)=0 \quad (28)$$

Therefore, the following relationships can be found

$${X_{3s}}=M_{inv}{}^{-1}(K_T Z_1+X_1+M_{inv}P_m+K_D X_2) \quad (29)$$

$$U\ =-K_s Z_2-\ \Gamma\widehat{\varphi}+M_{inv}\ Z_1-F_T+\dot{X}_{3s} \quad (30a)$$

$$U_f=G_T{}^{-1}(U-Lr) \quad (30b)$$

$$U\ =-K_s Z_2-\ \Gamma\widehat{\varphi}+M_{inv}\ Z_1-F_T+\dot{X}_{3s} \quad (30c)$$

$$({Z_2}^T\Gamma-\dot{\widehat{\varphi}}^T\gamma)=0\rightarrow\dot{\widehat{\varphi}}=\gamma^{-1^T}\Gamma Z_2 \quad (31)$$

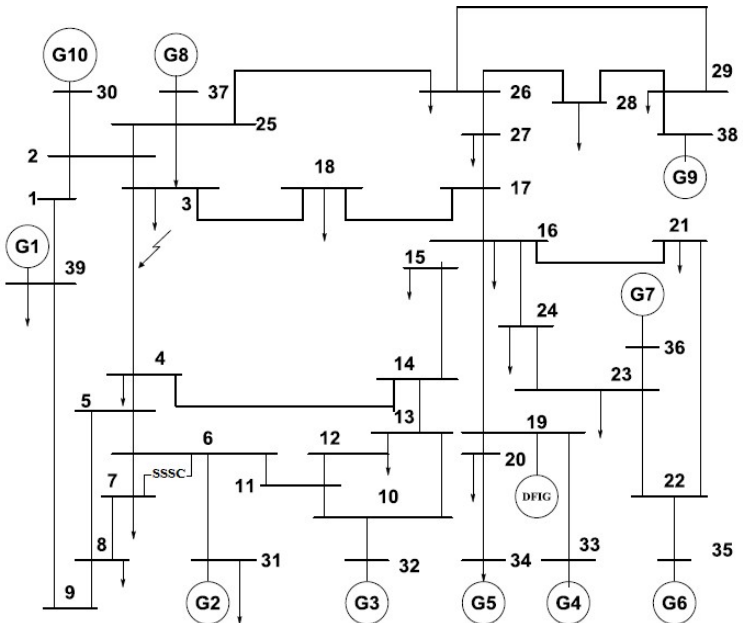

Fig. 7. The NEW ENGLAND standard 39-bus power system includes a wind generator equipped with DFIG

In (28), the definition of $\dot{x}_{3si}$ is as follows:

$$\begin{aligned}\dot{x}_{3si} =& M_i(1+k_{di}k_{Ti})x_{2i} - (k_{di}+k_{Ti})x_{3i} \\ &+ (k_{di}+k_{Ti})P_{mi}) - F_{Ti})\end{aligned} \tag{32}$$

Considering the stated conditions, the derivative of the Lyapunov function becomes negative semi-definite and as a result the stability of the system is proved [30, 31].

$$\dot{V}_L = -{X_1}^T K_D X_1 - {Z_1}^T K_T Z_1 - {Z_2}^T K_s Z_2$$

To better understand how the system and the designed controller work, a general diagram is shown in Fig. 5.

In the case of 2^{nd}-order model for synchronous generators, the internal voltage of the synchronous generators is constant, so the control inputs to improve the stability are DFIG input and SSSC related control signal.

The general design of the controller with applying 2^{nd}-order model for synchronous generators is the same as the design method which was proposed for 3^{rd} –order one. In the previous stage, the SSSC input is used to control the terminal voltage connected to it, however, here this control input is also designed using a backstepping method. Since the uncertain parameter is removed from the equations, the multi-input backstepping method is used without adaptation of the uncertain parameter. Considering the above changes, the general form of dynamic equations with respect to equation (24) is obtained as in (33):

$$\begin{cases} \dot{X}_1 = X_2 \\ \dot{X}_{2i} = M_{inv}[P_m - X_3] \\ \dot{X}_{3i} = F_T + G_T U \end{cases} \tag{33}$$

where $U = \begin{bmatrix} u_{d1} & r_1 \end{bmatrix}^T$, $G_{Tn} = \begin{bmatrix} G_T & L \end{bmatrix}$; r1 is the SSSC control input; u_{d1} is DFIG control input. Performing the design process as in the previous section and considering that the G_{Tn} matrix is a non-square matrix, the control input is obtained as follows:

$$U = ({G_{Tn}}^T G_{Tn})^{-1} {G_{Tn}}^T (-K_s Z_2 + M_{inv} Z_1 - F_T + \dot{X}_{3s} \tag{34}$$

3.2. Optimization of K_D, K_T and K_s Matrices Using PSO Intelligent Algorithm

In this sub-section, to obtain the best result to improve dynamic stability, the controller gain matrices are found using the PSO intelligent optimization algorithm. The objective function which is considered for this part is represented in (35). Minimizing the proposed objective function and obtaining the values of K_D, K_T and K_s matrices, the stability of the power system is improved [32–34]. The values for these matrices are given in Appendix D.

$$J = \int_{j=1}^{n} (\delta_i - \delta_{i0})^2 + \gamma \int_{j=1}^{n} (\omega_i - \omega_{i0})^2 \tag{35}$$

where γ is a weighting coefficient that can be determined experimentally. Extracting the optimal values for gain matrices in three different control modes (DFIG-only, SSSC-only and DFIG and SSSC simultaneous control) has been performed separately to improve dynamic stability.

3.3. Flowcharts of the Proposed Method to Improve Dynamic Stability of the Power System Including DFIG and SSSC

Regarding the modelling procedure developed in the previous section, the flowchart in Fig. 6 (a) depicts for the case that the synchronous generator is modelled with a 3^{rd} -order one. This model is applied and the control procedure is developed with DFIG and SSSC in different modes. Similarly, the flowchart in Fig. 6 (b) is related to the case, in which, the synchronous generator is modeled with 2^{nd}-order one, meaning that there are only control over DFIG and SSSC.

4. Simulation Results

To verify the performance of the proposed nonlinear control law and to see the effect of each of the DFIG and SSSC elements on the stability of the system in different modes, the NEW ENGLAND 39-bus network shown in Fig. 7 has been used. This network includes 10 synchronous machines, a DFIG on bus number 19 and a SSSC element between buses number 16 and 19, the specifications of this system are given in Appendix C.

It is assumed that in the selected network, a short circuit fault is occurred on bus number 4 for 100 milliseconds. Here, three cases are considered to investigate the effect of each element on stability.

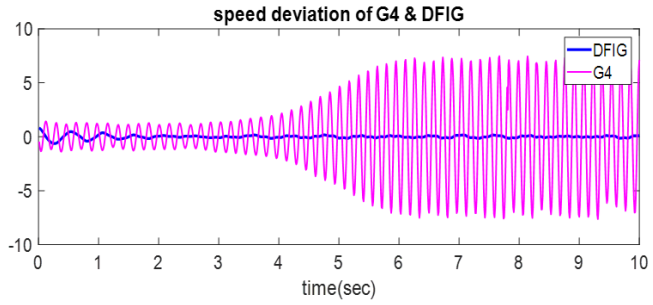

(a)

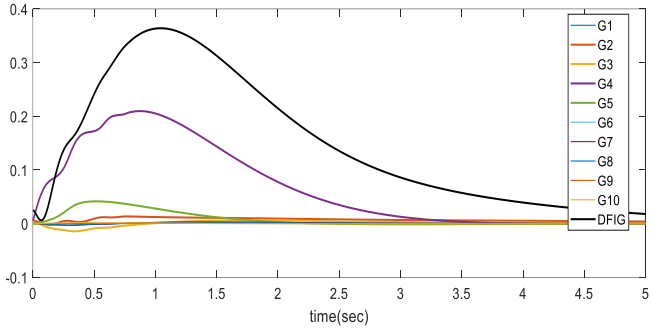

(b)

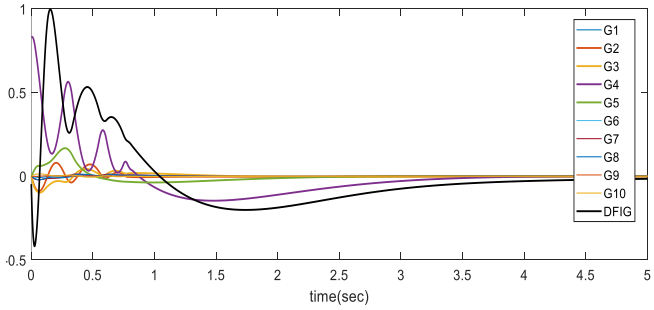

(c)

Fig. 8. (a) Speed deviation G4 and DFIG while is not control on system, (b) rotor angle deviation of all machines by only DFIG and excitation system of synchronous generator are multi input adaptive back stepping control, (c) speed deviation of all machines by only DFIG and excitation system of synchronous generator are multi input adaptive back stepping control

4.1. The First Scenario: Synchronous Generator with 3^{rd} Order Model

In this scenario, in the 39-bus network, a three-phase short circuit occurred near generator No. 4 for 100 milliseconds. Initially, the system does not have any control. For instance, the plot of the speed variations of the G4 and DFIG generators is typically shown in Fig. 8(a). It is clear that the power system is dynamically unstable. In the first study, the DFIG control inputs and synchronous generators are determined to improve the dynamic stability using the multi-input adaptive backstepping method. The SSSC control input is determined separately to improve the voltage profile by applying feedback linearization method. Figures 8(b) and 8(c) show the variations in the internal angles and speeds of the machines after clearing the fault in this case. As it turns out, all machines and DFIG have reached to their equilibrium condition.
In the second study, only the SSSC control input and the synchronous generators inputs are determined to improve the dynamic stability using the multi-input adaptive backstepping method, and the DFIG control input has no effect on control. In Figures 9 and 10, the variations in the rotor angles and speeds of

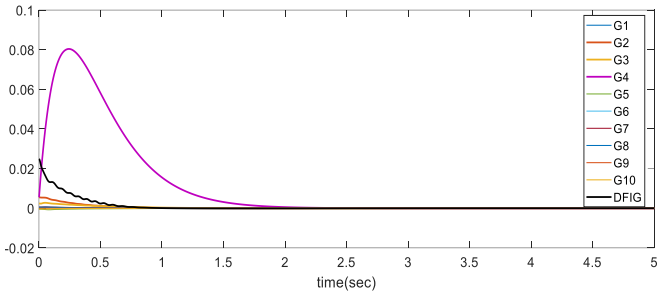

Fig. 9. Rotor angle deviation of the generators rotor after fixing the short circuit fault

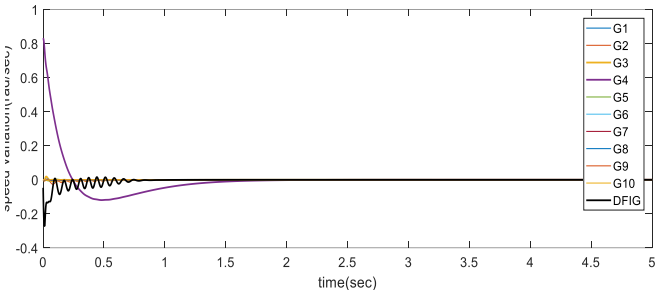

Fig. 10. Rotor speed deviation of the generators after the short circuit fault

the machines are depicted. It can be seen that these variations tend towards zero.

In the third study, in which the proposed method is fully applied, DFIG and SSSC control inputs with synchronous generators are simultaneously determined to improve dynamic stability using the multi-input adaptive backstepping method. In Figures 11, 12 and 13, speed variations, internal angle variations, and electrical power of the machines are shown. These variables have reached to their nominal values after a short transient part. In Table 2, the stability quantities such as settling time, overshoot value and rise time are compared to three states of primary condition. According to this table, the third case study behaves better than the previous two case studies. In other words, the damping rate is higher. In Table 3, a comparison is made between the proposed method in the third study with the results of [15]. The table shows that applying the proposed method results in better performance than the nonlinear method in [15]. Table 4 compares the proposed method under the same conditions to the linear method presented in [19], in which the proposed controller behaves even better.

To compare the damping characteristics of the proposed control method and validation of the quantities in Table 2, the phase diagrams for a number of machines such as G2, G4 and DFIG, in the three studies are shown in Fig. 14. The system starts from an initial point after clearing the fault, and reaches the equilibrium

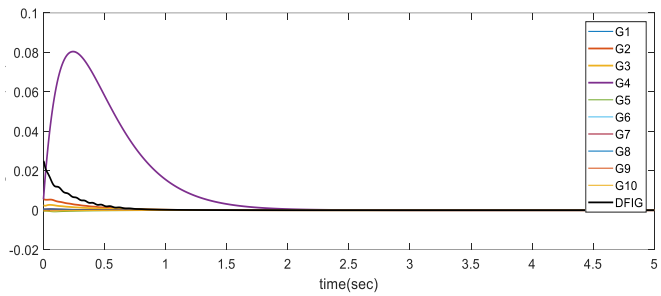

Fig. 11. Angle variation of the generators rotor after fixing the short circuit error in bus 39

Table 2. Comparison of control criteria in 3 state of primary case study for speed variation machines

	Only SSSC			Only DFIG			DFIG & SSSC simultaneously		
GEN NO	Overshoot percent	settling time (sec)	Overshoot (rad/sec)	settling time (sec)	Rise time (sec)	Rise time (sec)	Overshoot (rad/sec)	settling time (sec)	Rise time (sec)
3	0.025	0.25	.02	.24	0.048	0.05	0.1	1.6	0.4
4	0.12	1.8	.115	1.8	.24	0.25	0.15	2.4	0.92
5	0.01	0.11	.01	0.1	.029	0.03	0.2	2	0.2
DFIG	0.3	0.85	.35	0.75	.08	0.09	1	5	0.1

Table 3. Comparison of control criteria between adaptive multi input back-stepping and nonlinear control method in [15]

	Proposed control in this article Only DFIG State			Nonlinear Control design in [15]		
G3	Overshoot	settling time (sec)	Rise time (sec)	Overshoot	settling time (sec)	Rise time (sec)
Speed deviation	0.002p.u	4	0.3	0.005p.u	5	0.5
Rotor angle	14°	4	3	35°	5	0.1
Control signal	3.35 p.u	2.8	0.05	3.2 p.u	7.5	0.4

Table 4. Comparison of control criteria between adaptive multi-input back stepping and optimized linear control method in [19]

	Proposed control in this article with DFIG & SSSC			Optimized Linear Control Design in [19]		
G4	Overshoot	settling time (sec)	Rise time (sec)	Overshoot	settling time (sec)	Rise time (sec)
Speed deviation	0.002 p.u	3	0.15	0.015 p.u	4.5	0.2
Rotor angle	14°	3.5	1	55°	4	0.15
Control signal	3.35 p.u	2.8	0.05	-	-	-

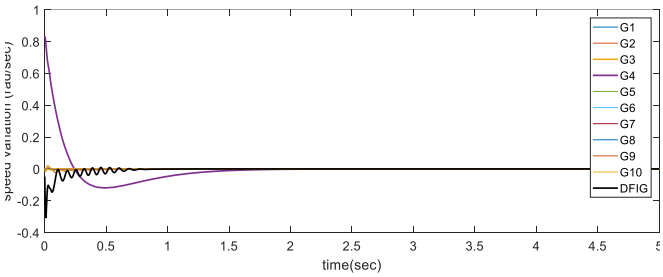

Fig. 12. Speed deviation of the generators after the short circuit fault in bus 39

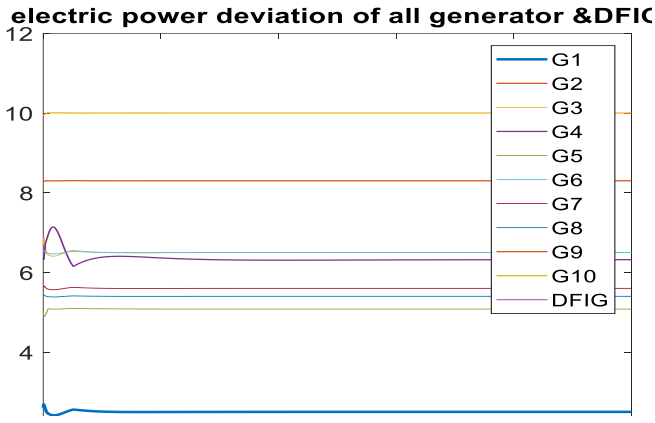

Fig. 13. Electric power of the generators and DFIG after the short circuit fault in bus 39

point. Figures 15 and 16 show the control signal and the results of parameter estimation in all three study modes. As shown in Fig. 15, the amplitude of the signals is limited and they have reached the same initial values. It can also be seen in Fig. 16 that the estimation error tends towards zero, i.e. the estimation of the parameters converges to the actual values. Also, in the third case, the responses look better than the two previous cases.

Due to the fact that the mechanical input power of the generators may change, it is considered that the mechanical input power of the DFIG suddenly changes by about 10% and then returns to its initial value. Fig. 17 shows the variations in angular velocity of generators for this test using the proposed control. It is observed that the controller acts well against these changes and stabilizes the system with the lowest time and oscillation amplitude.

Fig. 18 depicts the behavior of synchronous generator No. 4 in the case where the uncertain parameter related to Generator 4 increases by about 10% after clearing the fault. According to this figure, considering the parameter estimation in the control system, with the change of the uncertain parameter, the total response does not vary much and only the overshoot value is increased from 0.12 to 0.18 radians per second. This indicates the robustness of the control system to the changes in system uncertain parameters.

To demonstrate the robustness of the designed control system to changing the fault location, a three-phase short circuit fault is applied near machine No. 7. Fig. 19 shows the diagram of the speed variations of all generators after clearing this fault. It can be seen that all generators have stabilized after about 1.8 seconds.

4.2. The Second Scenario: Synchronous Generator with 2^{nd} -Order Model

This sub-section examines the stability of the power system when an unknown problem is occurred in the excitation system of synchronous generators for any reason and has no effect on the control of the generator. In this case, it is assumed that only the DFIG and SSSC elements are able to control and stabilize the power system. For this purpose, the model used for synchronous generators in this section is considered a 2^{nd}-order model. That is, the excitation system of synchronous generators is not active. In other words, the internal voltage amplitudes in synchronous generators are considered to be constant. Based on the proposed controller design method developed in Section 2–3, the SSSC and DFIG control inputs act simultaneously to improve the stability of the power system. Figures 20 to 23 show G4 rotor angle and speed variations, and phase diagrams, respectively. According to these figures, in this simulation mode, the controller is able to

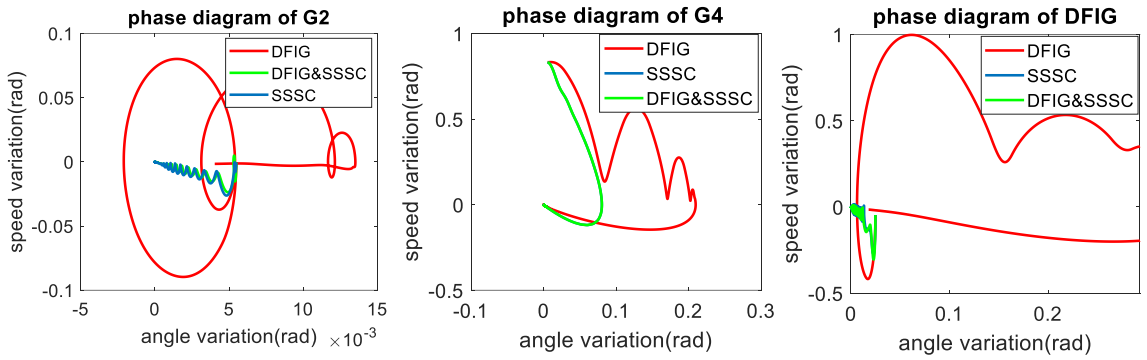

Fig. 14. Phase diagram of wind turbine based DFIG and G4 and G2

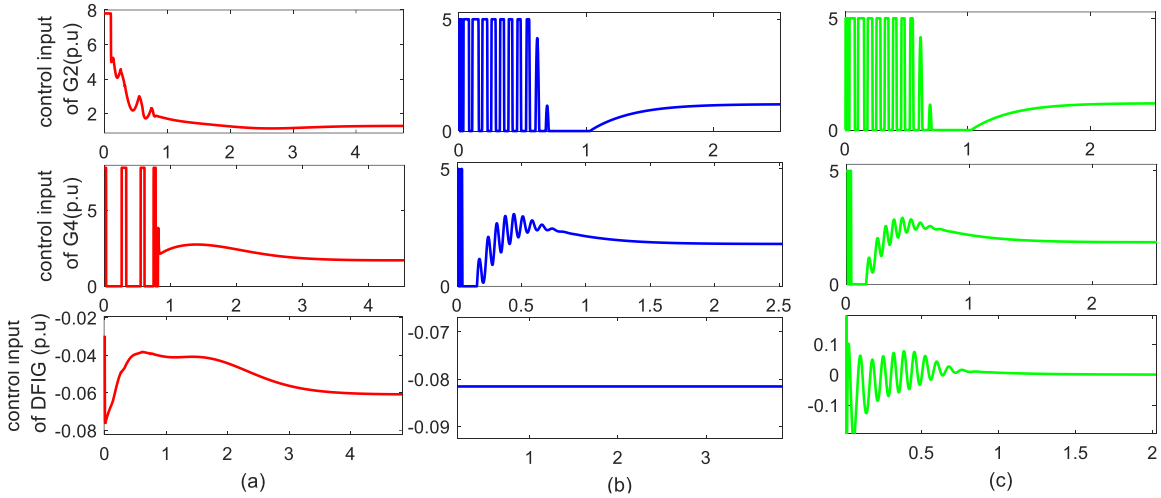

Fig. 15. Control signals of G2, G4 and DFIG (a) DFIG and excitation system control signals are designed by Multi input adaptive back stepping control, (b) SSSC and excitation system control signals are designed by Multi input adaptive back stepping control, (c) DFIG, SSSC and excitation system control signals are designed by Multi input adaptive back stepping control

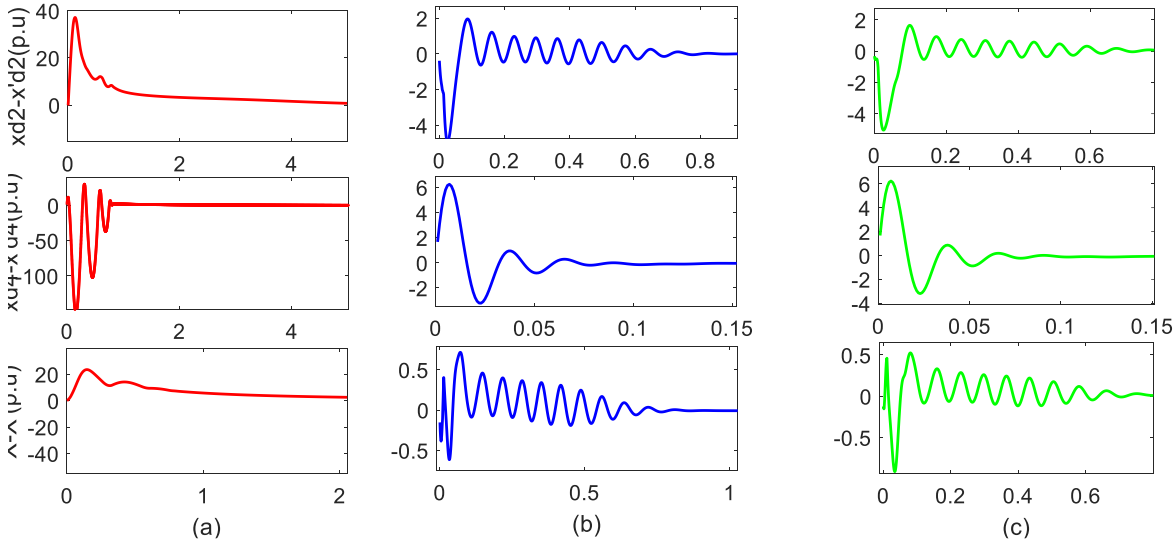

Fig. 16. Estimation deviation for G2, G4 and DFIG, (a) DFIG and excitation system control signals are designed by Multi input adaptive back stepping control, (b) SSSC and excitation system control signals are designed by Multi input adaptive back stepping control, (c) DFIG, SSSC and excitation system control signals are designed by Multi input adaptive back stepping control

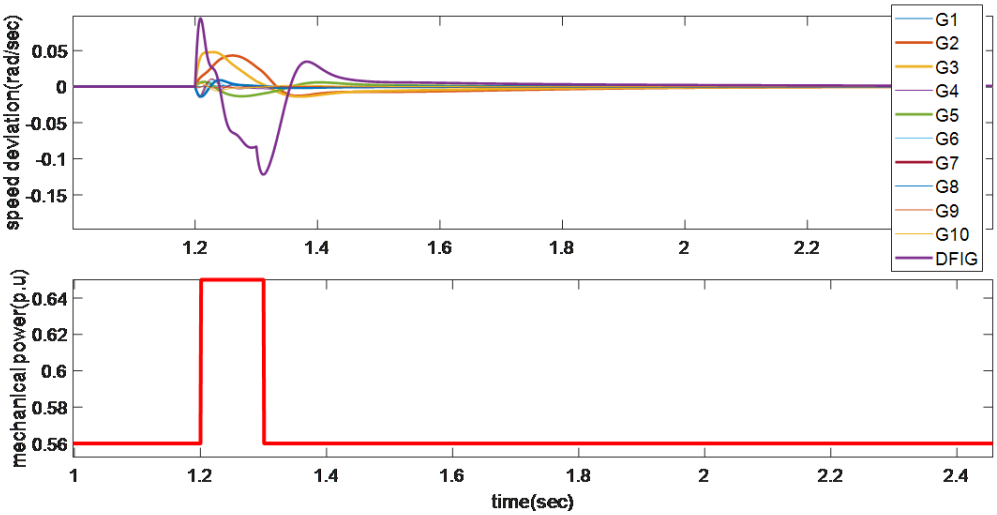

Fig. 17. Speed deviations of synchronous generators and DFIG considering 10% mechanical power variation in DFIG

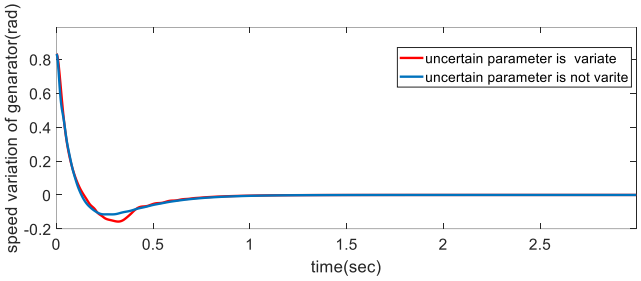

Fig. 18. Speed deviation of G4 against changing uncertain parameter

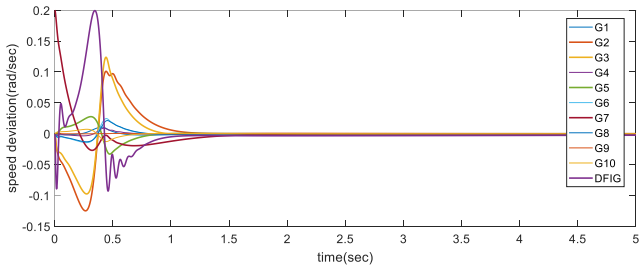

Fig. 19. Speed deviations of synchronous generators and DFIG against changing point of fault occur to near G7

stabilize the system, but the overshoot and settling times as well as the amount of fluctuations and the steady-state error have been increased compared to the first scenario. The reason is that there is no control over the generators. For this case, it is concluded that stabilization is just as significant. This fact shows the strength of the proposed method in damping the amplitude of fluctuations.

5. Conclusions

In this study, an adaptive multi-input backstepping controller is designed for power systems including DFIG and SSSC. The final designed control law makes the control system robust against parameter changes with a limited value for control signals amplitude by estimating the uncertain parameters related to synchronous generators and DFIG.

The controller is designed by considering the appropriate variables for applying the backstepping method and selecting a suitable positive-definite Lyapunov function which guarantees the stability of the power system. According to the results obtained

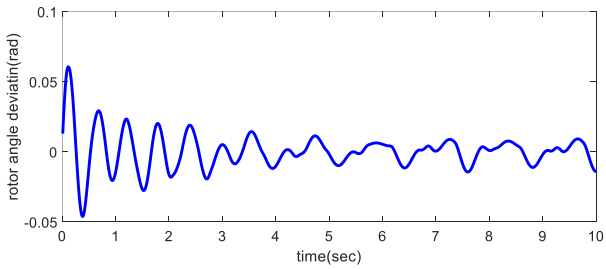

Fig. 20. Rotor angle deviation of G4 the after clearing the short circuit fault

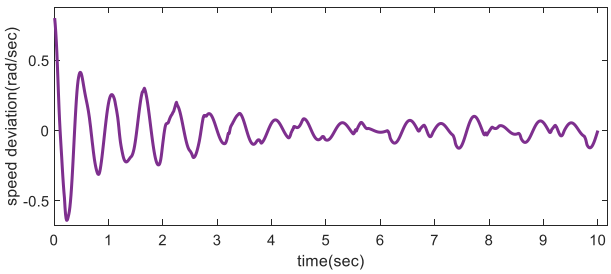

Fig. 21. Speed deviation of G4 the after fixing the short circuit fault

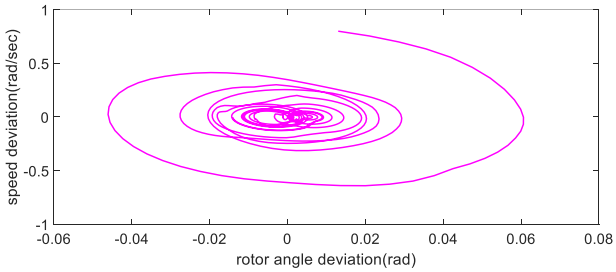

Fig. 22. Phase diagram of G2, G4 and wind turbine based DFIG

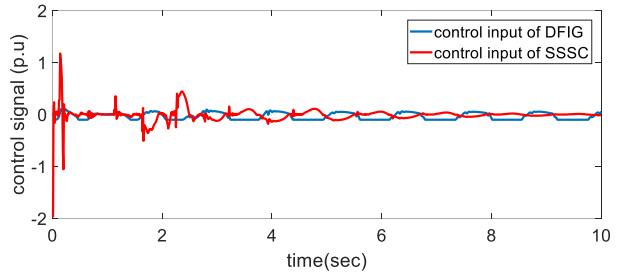

Fig. 23. Control signals of synchronous generators and DFIG

from Table 3, the overshoot value and the amount of settling time are improved about 50% and 20%, respectively, compared to the nonlinear methods in the latest studies. In addition, it has a better performance than the linear methods developed in the existing literature. Moreover, the proposed control is robust against parameters changes, load changes and relocation of disturbances.

Finally, in the pessimistic state that the generators do not act, the adaptive backstepping control on DFIG and SSSC, which is performed by PSO optimization, works adequately well in damping the amplitude of fluctuations after the occurrence of disturbances.

APPENDIX

Appendix A. Parameters and variables definitions of section 3

$$\begin{bmatrix} a_{1,1} & a_{1,2} & \dots & a_{1,n} \\ a_{2,1} & a_{2,2} & \dots & a_{2,n} \\ . & . & . & . \\ a_{n,1} & a_{n,1} & \dots & a_{n,n} \end{bmatrix} \begin{bmatrix} \dot{V}_1 \\ \dot{V}_2 \\ \vdots \\ \dot{V}_n \\ \dot{\phi}_2 \\ \vdots \\ \dot{\phi}_n \end{bmatrix} \begin{matrix} \\ \\ \\ \\ \dot{\phi}_1 \\ \\ \\ \end{matrix} =$$

$$- \begin{bmatrix} a_{1,1} & a_{1,2} & \dots & a_{1,n} \\ a_{2,1} & a_{2,2} & \dots & a_{2,n} \\ . & . & . & . \\ a_{n,1} & a_{n,1} & \dots & a_{n,n} \end{bmatrix} \begin{bmatrix} \dot{E'}_{q1} \\ \dot{E'}_{q2} \\ \vdots \\ \dot{E'}_{qn} \\ \dot{\delta}_2 \\ \vdots \\ \dot{\delta}_n \end{bmatrix} \begin{matrix} \\ \\ \\ \\ \dot{\delta}_1 \\ \\ \\ \end{matrix}$$

$$a_{i,j} = \sum_{i=1}^{n}\sum_{j=1}^{n} V_j(G_{ij}cos(\theta_i-\theta_j) + B_{ij}sin(\theta_i-\theta_j))$$

$$a_{i,j+N} = \sum_{i=1}^{n}\sum_{j=1}^{N} V_iV_j(-G_{ij}sin(\theta_i-\theta_j) + B_{ij}cos(\theta_i-\theta_j)\ )$$

$$a_{i+N,j} = \sum_{i=1}^{n}\sum_{j=1}^{N} V_j(G_{ij}sin(\theta_i-\theta_j) - B_{ij}cos(\theta_i-\theta_j)$$

$$\begin{aligned} a_{i+N,j+N} =& \sum_{i=1}^{n}\sum_{j=1}^{N} V_iV_j(G_{ij}cos(\theta_i-\theta_j) \\ &+ B_{ij}sin(\theta_i-\theta_j)\ )\ b_{i,i} \\ =& \frac{\acute{E}_{qi}V_icos(\delta_i-\theta_i)}{\acute{x}_{di}} \\ &- \frac{{V_i}^2cos2(\delta_i-\theta_i)(\acute{x}_{di}-x_{qi})}{\acute{x}_{di}x_{qi}} \end{aligned}$$

$$b_{i,i+n} = \frac{V_isin(\delta_i-\theta_i)}{\acute{x}_{di}}$$

$$\begin{aligned} b_{i+N,i} =& \frac{-\acute{E}_{qi}V_isin(\delta_i-\theta_i)}{\acute{x}_{di}} \\ &- \frac{2{V_i}^2cos(\delta_i-\theta_i)sin(\delta_i-\theta_i)\ (\acute{x}_{di}-x_{qi})}{\acute{x}_{di}x_{qi}} \end{aligned}$$

$$b_{i+N,i+n} = \frac{V_icos(\delta_i-\theta_i)}{\acute{x}_{di}}$$

$$g_{i,1} = V_i(G_{i,j}cos\theta_i + B_{ij}sin\theta_i)$$

$$g_{i,2} = V_i(G_{i,j}sin\theta_i - B_{ij}cos\theta_i\ )$$

$$g_{i+N,1} = V_i(G_{i,j}sin\theta_i - B_{ij}cos\theta_i)$$

$$g_{i+N,2} = -V_i(G_{i,j}cos\theta_i + B_{ij}sin\theta_i)$$

$$f_{gi}(x) = \frac{1}{\acute{T}_{d0i}}(-\frac{\acute{E}_{qi}x_{di}}{\acute{x}_{di}} + \frac{V_i(x_{di}-\acute{x}_{di})cos(\delta_i-\theta_i)}{\acute{x}_{di}})$$

$$g_{gi}(x) = \frac{1}{\acute{T}_{d0i}}$$

$$\begin{aligned} f_{di}(x) =& \frac{1}{T_{0i}}\Big[-\frac{X_i}{\acute{X}_i}\acute{E}_i + \frac{X_i-\acute{X}_i}{\acute{X}_i}V_icos(\delta_i-\theta_i) \\ &- \frac{cos(\delta_i)T_{0i}\acute{E}_i}{sin(\delta_i)}(\omega_s-\omega_0) - \frac{V_icos(\delta_i)sin(\delta_i-\theta_i)}{sin(\delta_i)}\frac{X_i-\acute{X}_i}{\acute{X}_i}\Big] \end{aligned}$$

$$g_{di}(x) = \frac{\omega_s}{sin(\delta_i)}$$

$$u_{d1i} = V_{ri}cos(\Phi_{ri})$$

$$u_{d2i} = V_{ri}sin(\Phi_{ri})$$

Appendix B. Variables definitions of section 4

$$\begin{aligned} f_{TN} =& B_wf_{dw}V_wsin(\delta_i-\theta_i) + B_w\acute{E}_wV_w(\omega_w-\omega_{w0})cos(\delta_w-\theta_i) \\ &+ B_w\acute{E}_wsin(\delta_i-\theta_i)\sum_{j=1}^{2n}c_{wj}H_j \\ &- B_w\acute{E}_wV_wcos(\delta_w-\theta_i)\sum_{j=1}^{2n}c_{(w+n1),j}H_j \end{aligned}$$

$$\begin{aligned} M =& Bg_{di}V_isin(\delta_i-\theta_i)u_{d1i} + B\acute{E}_isin(\delta_i-\theta_i)\Big[\sum_{j=1}^{n1}d_{ij}u_{sj} \\ &+ \sum_{j=1}^{n2}d_{i,j+n1}u_{d1j} + k_{i,1}r\Big] - B\acute{E}_iV_icos(\delta_i-\theta_i) \\ &\Big[\sum_{j=1}^{n1}d_{(i+n+2),j}u_{sj} + \sum_{j=1}^{n2}d_{(i+n+2),j+n1}u_{d1j}\Big] \end{aligned}$$

Appendix C. Specification of new England 39 bus and 10 machine power system

Table 5. Equivalent specifications of wind turbine based DFIG

X_d	$X_d^{'}$	X_q	H
2.605	0.107	0.0107	4

Table 6. Equivalent specifications synchronous generators

Unit No.	H	Ra	x'd	x'q	xd	xq	T'do	T'qo	xl
1	5	0	0.006	0.008	0.02	0.019	7	0.7	0.03
2	30	0	0.0697	0.170	0.295	0.282	6.56	1.5	0.035
3	35.8	0	0.0531	0.0876	0.2495	0.237	5.7	1.5	0.0304
4	28.6	0	5 26.0	0 0.132	0.166	0.67	0.62	5.4	0.44
5	26	0	0.132	0.166	0.67	0.62	5.4	0.44	0.054
6	34.8	0	0.05	0.0814	0.254	0.241	7.3	0.4	0.0224
7	26.4	0	0.049	0.186	0.295	0.292	5.66	1.5	0.0322
8	24.3	0	0.057	0.0911	0.290	0.280	6.7	0.41	0.028
9	34.5	0	0.057	0.0587	0.2106	0.205	4.79	1.96	0.0298
10	42	0	0 0.031	0.008	0.1	0.069	10.2	0.0	0.0125

Appendix D. DFIG and SSSC Control Parameters

$$K_D = Diag\begin{bmatrix} 51.992 & 17.934 & 41.124 & 70.78 & 24.714 & 87.88 & 29.55 & 108.71 & 69.11 & 91.65 & 27.81 \end{bmatrix}$$
$$K_T = Diag\begin{bmatrix} 32.97 & 10.98 & 69.28 & 71.28 & 70.41 & 51.12 & 77.34 & 58.28 & 88.01 & 63.089 & 110.44 \end{bmatrix}$$
$$K_S = Diag\begin{bmatrix} 24.69 & 81.06 & 26.83 & 2.307 & 63.509 & 53.149 & 57.65 & 69.39 & 92.35 & 34.62 & 79.281 \end{bmatrix}$$

Only SSSC control parameter:

$$K_D = Diag\begin{bmatrix} 38.807 & 35.402 & 11.06 & 37.14 & 89.75 & 54.01 & 74.22 & 49.45 & 10.72 & 48.26 & 84.37 \end{bmatrix}$$
$$K_T = Diag\begin{bmatrix} 36.60 & 28.13 & 32.36 & 40.99 & 72.0 & 77.11 & 32.06 & 86.00 & 78.99 & 55.12 & 88.51 \end{bmatrix}$$
$$K_S = Diag\begin{bmatrix} 12.19 & 74.77 & 1.22 & 24.46 & 81.83 & 8.83 & 65.01 & 24.94 & 53.53 & 70.618 & 80.174 \end{bmatrix}$$

REFERENCES

[1] Y. Wang, T. Huang, X. Li, J. Tang, Z. Wu, Y. Mo, L. Xue, Y Zhoe, T. Niu, S. Sun, "A Resilience Assessment Framework for Distribution Systems Under Typhoon Disasters," IEEE Access, Vol. 9, Nov 2021.

[2] S. Muller, M. Deicke, R. W. De Doncker, "Doubly-fed induction generator systems for wind turbines", *IEEE Ind. Appl. Mag.*, June 2002.

[3] A. Hasanzadeh, H. Shayeghi, S. R. Mousavi-Aghdam, "A New Fuzzy Direct Power Control of Doubly-Fed Induction Generator in a Wind Power System", *J. Oper. Autom. Power Eng.*, vol. 10, no. 3, pp. 179-188, Dec. 2022.

[4] Y. Bostani, S. Jalilzadeh, "A New Approach based on Wide-Area Fuzzy Controller for Damping of Sub Synchronous Resonance in Power System including DFIG", *J. Oper. Autom. Power Eng.*, vol. 11, no. 1, pp. 61-68, Apr. 2023.

[5] E. Hosseini, N. Behzadfar, M. Hashemi, M. Moazzami, M. Dehghani, "Control of Pitch Angle in Wind Turbine Based on Doubly Fed Induction Generator Using Fuzzy Logic Method", *Journal of Renewable Energy Environ.*, vol. 9, no. 2, pp. 1-7, 2022.

[6] J. Ma, Y. Zhou, Y. Shen, Y. Du, J. Wang, S. Sun, Y. Huang, S. Zhao, "Study on the energy stability region of DFIG-integrated power system with virtual inertia", *IET Renew. Power Gener.*, vol. 16, pp. 2020–2035, 2022.

[7] L. Jiao, B.T. Ooi , G. Joos, F. Zhoub, "Doubly-fed induction generator (DFIG) as a hybrid of asynchronous and synchronous machines", *Electric Power Syst. Research*, vol. 76, pp: 33–37, 2005.

[8] H. S. Koa, G. G. Yoonb, N. H. Kyunga, W. P. Hongc, "Modeling and control of DFIG-based variable-speed wind-turbine", *Electric Power Syst. Research*, vol. 78, pp:1841–1849, 2008.

[9] N. G. Hingorani and L. Gyugyi, Understanding FACTS, Concepts and Technology of Flexible AC Transmission Systems, Wiley-IEEE Press, 2000.

[10] A. Saleem Mir and N. Senroy, "DFIG damping controller design using robust CKF based adaptive dynamic programming", *IEEE Trans. Sustainable Energy*, vol. 11, no. 2, pp. 839–850, 2018.

[11] P. R. Sahu, P. K. Hota, S. Panda, "Power system stability enhancement by fractional order multi input SSSC based controller employing whale optimization algorithm", *J. Electr. Syst. Inf. Technol.*, vol. 5, no 3, pp. 326-336 , December 2018.

[12] P. Kundur, Power System Stability and Control, New York, NY, USA: McGraw-Hill, 1994.

[13] W. Du, X. Chen, H, Wang, "Parameter tuning of the PLL to consider the effect on power system small-signal angular stability", *IET Renewable. Power Gener.*, vol. 12, no. 1, pp. 1-8, 2018.

[14] Y. Liu, Q. H. Wu, H. Kang, X. Zhou, " Switching Power System Stabilizer and Its Coordination for Enhancement of Multi-machine Power System Stability", *J. Power Energy syst.*, vol. 2, no. 2, June 2016.

[15] T. K. Roy, M. A. Mahmud, A. M. T. Oo, "Robust Adaptive Backstepping Excitation Controller Design for Higher-Order Models of Synchronous Generators in Multi machine Power Systems", *IEEE Trans. Power Syst.* , vol. 34, no. 1, 2019.

[16] M. A. Mahmud, M. J. Hossain, H. R. Pota, and A. M. T. Oo ," Robust Partial Feedback Linearizing Excitation Controller Design for Multimachine Power Systems", *IEEE Trans. Power Syst.* , vol. 32, no. 1, pp. 3-16, 2017.

[17] F. Poitiers , T. Bouaouiche, M. Machmoum, "Advanced control of a doubly-fed induction generator for wind energy conversion", *Electr. Power Syst. Res.* , vol. 79, no. 7. pp. 1085–1096, 2009.

[18] T. Parida, S. Dhar, N. Nayak, "A finite time adaptive back-stepping sliding mode control for instantaneous active-reactive power dynamics based DFIG-wind generation towards improved grid stability ", *Wind Energy*, vol. 23, no. 12, 2020 .

[19] M. Maleki, S.Abazari, "Dynamic Stability Improvement of Power System With Simulation and Coordinated Control of DFIG and UPFC using LMI", *Int. J. Indust. Electron. Control Optimiz.*, vol. 4, no. 3, pp.341-353, July 2021.

[20] J. Ma, Y. Qiu, Y. Li, W. Zhang, Z. Song, J. S. Thorp, "Research on the Impact of DFIG Virtual Inertia Control on Power System Small-Signal Stability Considering the Phase-Locked Loop", *IEEE Trans. Power Syst.*, vol. 32, no.

3, pp. 2094 - 2105, 2016.
[21] S. Kamel, B. Mansour, B. Faouzi, "Enhancement of DFIG Operation Using a STATCOM Under a Voltage Grid Faults", 8^{th} Int. Conf. Control, Decision and Information Techno. (CoDIT), Istanbul, Turkey, 2022.
[22] A. Sunil, M. Shahin, "Improving the Voltage Stability of Power System Connected with Wind Farm Using SSSC", Int. Conf. Communi. Control Infor. Sciences (ICCISc), Idukki, India, 2021.
[23] J. Alnasseir, R. Alcharea, F. Almaghout, "Improving the Stability of Smart Grids by Using Flexible Alternating Current Transmission Systems (FACTS)", 12^th Int. Renewable Eng. Conf. (IREC), Amman, Jordan, 2021.
[24] A. Movahedia, A. Halvaei Niasara, G. Gharehpetianb, " Designing SSSC, TCSC, and STATCOM controllers using AVURPSO, GSA, and GA for transient stability improvement of a multi-machine power and GA for transient stability improvement of a multi-machine power system with PV and wind farms system with PV and wind farms", Electri. Power Energy Syst., vol. 106 , pp. 455–466, 2019.
[25] K. Elkington, V. Knazkins, M. Ghandhari, "On the stability of power systems containing doubly fed induction generator-based generation", *Electric Power Syst. Research*, vol. 78, no. 9 , pp. 1477–1484, September 2008.
[26] M. Noroozian, M. Ghandehari, "Improving Power System Dynamics By Series-Connected FACTS Device", *IEEE Trans. Power Delivery*, vol. 12, no. 4, October 1997.
[27] J. Ma, D. Zhao, Y. Shen and A. G. Phadke, "Research on Positioning Method of Low Frequency Oscillating Source in DFIG-Integrated System with Virtual Inertia Control", *IEEE Trans. Sustainable Energy*, vol. 11, no. 3, pp. 1693 – 1706, 2020.
[28] G. S. Kaloi, M. Hussain, "Dynamic Modeling and Control of DFIG for Wind Energy Conversion System Using Feedback Linearization ", *J. Electri. Eng. Techno.*, vol. 11, no. 5, pp. 1137-1146, September 2016.
[29] Z. Ding, Nonlinear and Adaptive Control Systems, IET Control Engineering Series 84, Published by The Institution of Engineering and Technology, London, United Kingdom, 2013.
[30] H. K. Khalil, Nonlinear systems, Upper Saddle River, NJ: Prentice Hall, 2002.
[31] E. Slotine, W. Li, Applied Nonlinear Control, Published by Prentice Hall, 1991.
[32] Y. Chi, Y. Xu,"Multi-objective robust tuning of STATCOM controller parameters for stability enhancemnt of stochastic wind-penetrated power systems", *IET Gener. Transm. Distrib.* , vol. 14, no. 21, pp. 4805-4814, September 2020.
[33] B. K. Dubey, N. K. Singh , "Multi machine power system stability enhancement with UPFC using linear quadratic regulator techniques", *Int. J. Advanced Research Eng. Techno.*, vol. 11, no. 4, pp. 219-229, April 2020.
[34] A. Sabo, N. I. Abdul Wahab, M. L. Othman, M. Zurwatul, A. M. Jaffar, H. Beiranvand, "Optimal design of power system stabilizer for multimachine power system using farmland fertility algorithm", *Electri. Energy Syst.*, vol. 30, no. 12, 2020.